EUROPEAN ORGANIZATION FOR NUCLEAR RESEARCH

CERN-PPE/91-203
7 October 1991

MEASUREMENT OF THE ANALYSING POWER OF THE CHARGE-EXCHANGE $\bar{p}p \rightarrow \bar{n}n$ REACTION IN THE MOMENTUM RANGE 546–875 MeV/*c* AT LEAR

R. Birsa, F. Bradamante, A. Bressan, S. Dalla Torre-Colautti, M. Giorgi,
M. Lamanna, A. Martin, A. Penzo, P. Schiavon, F. Tessarotto,
INFN Trieste and University of Trieste, Italy

M.P. Macciotta, A. Masoni, G. Puddu, S. Serci,
INFN Cagliari and University of Cagliari, Italy

T. Niinikoski, A. Rijllart,
CERN, Geneva, Switzerland

A. Ahmidouch, E. Heer, R. Hess, C. Lechanoine-Le Luc, C. Mascarini, D. Rapin,
DPNC, University of Geneva, Switzerland

J. Arvieux, R. Bertini, H. Catz, J.C. Faivre, R.A. Kunne, F. Perrot-Kunne,
DAPNIA and LNS, CEN Saclay, Gif-sur-Yvette, France

M. Agnello, F. Iazzi, B. Minetti,
INFN Turin and Turin Polytechnic, Turin, Italy

T. Bressani, E. Chiavassa, N. De Marco, A. Musso, A. Piccotti,
INFN Turin and University of Turin, Italy

Abstract

Results are given for the analysing power of the $\bar{p}p \rightarrow \bar{n}n$ charge-exchange reaction at four incident beam momenta. The measurement is part of an experimental programme to study the spin structure of this reaction at LEAR. The analysing power shows strong angular and energy dependence, which at present is not reproduced by the existing meson-exchange potential models.

(Submitted to Physics Letters B)

We have measured at eight $\bar{p}$ momenta the analysing power A_{0n} in the $\bar{p}p \to \bar{n}n$ charge-exchange reaction, from 608 to 1306 MeV/c incident beam momentum, in steps of 100 MeV/c, using a solid polarized target. Results at 704 MeV/c have already been published [1], and preliminary results at other momenta have been illustrated at several conferences [2–4]. In this paper we give final results at 608, 804, and 905 MeV/c incident $\bar{p}$ momenta. Compared with [Ref. 1], the analysis of the data has been improved, leading to some reduction of the errors. Consequently for completeness, the results of the improved analysis are given also at 704 MeV/c.

As discussed in [Ref. 1], the charge-exchange reaction is expected to be a particularly sensitive channel to probe the nucleon–antinucleon force. The data given in this paper provide, for the first time, a scan of A_{0n} in the energy range below the one-pion threshold, where the potential model approach has proved to be very effective in other reactions.

The experiment (PS199) has been carried out at the CERN Low Energy Antiproton Ring (LEAR), using the extracted beam line C1, with a typical intensity of 1–2 $\times$ 10^6 $\bar{p}$/s.

The measurement has been performed detecting both the $\bar{n}$ and the n produced in the reaction, and the events on the polarized free hydrogen of the target have been identified using the times-of-flight (TOF) and the measured space coordinates of all the particles. Furthermore, the apparatus has been designed to give a very good $\bar{n}$–n separation, which is necessary for an unambiguous determination of the scattering angle of each event.

The layout of the experiment is shown in Fig. 1; rather detailed descriptions of the apparatus have been given elsewhere [1, 4], so here just a short presentation will be given for completeness. The neutron detectors are NC1, NC2 and NC3, and ANC1 and ANC2 are the antineutron detectors. The dashed line indicates the $\bar{p}$ beam direction. The target sits in the nose of a 1 m long cryostat (shown in the figure together with the polarized target magnet PTM), and to reach the target the beam travels along its axis. Two scintillation counters define the beam; counter B0 is located just before the cryostat; the other counter, B12, is placed inside the cryostat, 19 cm from the target centre.

The pentanol polarized target (PT), 12 cm long, is operated in the frozen-spin mode [5] and a very high polarization (about 90%) can be achieved in 2–3 hours; with the holding magnetic field of 3.785 kG, the polarization decay is about 2% per hour. During data taking, the target polarization was about 80%, and, to reduce systematic effects, the spin orientation was reversed every four one-hour spills. For background evaluation, the PT was replaced by a dummy target (DT), having the same mass and density as the PT, but no hydrogen. The azimuthal acceptance (±15°) is limited by the magnet coils. To reject annihilation

and elastic events at trigger level, the target region is surrounded by a scintillator veto counter. A forward veto counter (FV) vetoes the non-interacting forward-going $\overline{p}$'s.

The NC detectors [6] are made up of a total of 53 vertical scintillation counters. Each scintillator is 8 cm wide and 20 cm thick; their lengths were chosen between from 40 and 130 cm according to the scattering angle. Each bar is viewed from each end by a photomultiplier (PM).

Each ANC counter [7] is made up of a succession of five modules, each made of four planes, of limited streamer tubes (LST), separated by 3 cm thick iron slabs. When an annihilation occurs in any of these iron slabs, the two telescopes of LST planes surrounding the slab are used to detect the tracks of the charged products of the annihilation, which show a characteristic "star" pattern. Each module has a sensitive surface of 166×200 cm^2 and also includes one hodoscope of scintillation counters for triggering purposes, and for the TOF measurement.

A charge-exchange trigger was given by the coincidence:

$$(B0 \cdot B1 \cdot B2) \cdot (NC1 \cdot ANC1 + (NC2 + NC3) \cdot ANC2)$$

and no signal in the veto counter box surrounding the target. NC means that at least one bar was hit, and ANC that at least two scintillators were hit in the corresponding detector.

The data at 704, 804, and 905 MeV/c have been collected in the same 8-day run. At the end of this run, the PT has been replaced by the DT; the background data have been taken at 704 and 905 MeV/c. The data at 608 MeV/c have been collected in a later period (May 1990), together with data at higher momenta (1005, 1106, 1207, and 1307 MeV/c), whose analysis is in progress. In this second run, some improvements were made to the data acquisition system, so that the amount of "useful beam" (i.e. the integrated beam entering the target during the data taking) could be almost doubled (typically it went from 2×10^{10} to 4×10^{10} $\overline{p}$'s).

In the off-line analysis, as a first step, the $\overline{n}$ candidates are identified by requiring, in the two LST modules sandwiching any of the four iron slabs, at least three tracks meeting in a common point, in the horizontal (or vertical) projection, and at least two tracks with the same vertex in the other projection. This selection allows us to identify the $\overline{n}$'s with an efficiency of about 20%. The probability of misidentifying a neutron as an $\overline{n}$ has been measured to be smaller than 10^{-4}. In the sample of the events with an $\overline{n}$ candidate (about 10% of the total sample), neutrons are identified by requiring that at most two adjacent bars be hit in the NC hodoscopes. The neutron coordinates are given by the bar number

(horizontal) and by the difference between the time given by the top and the bottom PM of each bar (vertical).

In the analysis of the data of Refs [1] and [4], the directions of the two particles were computed using the neutron coordinates, the $\bar{n}$ annihilation point, the centre of the target, and the average beam direction. The charge-exchange events on hydrogen were selected on the basis of coplanarity, angular correlation, and cuts on both TOFs.

In the present work, the charge-exchange events are identified on the basis of the χ^2 of a global 3-C kinematical fit of all the measured quantities, i.e. the transverse coordinates of the n and the $\bar{n}$ on their corresponding detectors, the beam position and direction on B12, and the n and the $\bar{n}$ TOF. The fit allows the determination of the only unknown coordinate, the $\bar{p}$ interaction vertex coordinate along the beam direction (z_{vtx}), with a precision of about 4 cm. Moreover, the fit allows:

– a better determination of θ_{cm}, the scattering angle in the centre-of-mass system (calculated from the coordinates of the forward-going particle in the previous analysis).

– a reduction of the background-to-signal ratio by about a factor of two.

The χ^2 distribution for the events in the target region ($|z_{vtx}| < 15$ cm) is shown in Fig. 2a for the PT and the DT events (hatched histogram), at 875 MeV/c. The charge-exchange events on hydrogen show up very clearly as the large peak at low χ^2. The tail of the χ^2-distribution for the PT lies somewhat higher than that of the DT events: a certain fraction (about 10%) of the $\bar{n}$ suffer small-angle scattering when going through the NC counter in front of the ANC detector, thus giving no signal in the NC, which otherwise would act as a veto to reject the event. The position of the cut ($\chi^2 = 20$) applied to select the charge-exchange events on hydrogen has been chosen to accept as many of these events as possible, whilst keeping the background down to a reasonable level. In Fig. 2, we give the distribution of $|z_{vtx}|$, for $\chi^2 < 20$, for the events of the two targets. Some good events are produced on the hydrogen content of the B12 and on the FV scintillation counters (their position along the z-axis is indicated in the figure), and they contribute to almost 50% of the background at low χ^2.

For the final analysis, we choose the cuts $\chi^2 < 20$ and $|z_{vtx}| < 15$ cm. With these cuts, comparing the events obtained with the PT target (hydrogen and nuclear content), and with the DT (nuclear content only), we derive the ratio $f = B/(B + S)$, where B and S indicate the background and the signal, i.e. the accepted charge-exchange events on unpolarized and polarized protons of the PT, respectively. Figures 2c and 2d show values of f as a function of $\cos\theta_{cm}$ at the two momenta where data were collected also with the DT. The best fits obtained,

assuming a $\sin^2 \theta_{cm}$ dependence, are also shown. Values of f at the other two beam momenta (p) were obtained by interpolation, assuming a $1/p^2$ dependence.

Figure 3 shows the measured angular distribution of the analysing power A_{0n} at the four momenta: 546, 656, 767, and 875 MeV/c. These are the mean values of the $\bar{p}$ momentum in the PT when the momentum of the extracted beam from LEAR was 608, 704, 804, and 905 MeV/c respectively (owing to the considerable amount of target material, the reaction momentum ranges were 497–588, 622–688, 740–790 and 854–895 MeV/c). The error bars are statistical. Numerical values are given in Table 1. Only the data taken when the beam transmission through the target, defined by the ratio (B0 · B1 · B2)/B0, was stable within ±5%, have been used to evaluate A_{0n}. Systematic effects due to variations of the $\bar{p}$ beam intensity have been investigated, and found to be smaller than the statistical fluctuations. The polarization calibration has an absolute uncertainty of ±4%, which acts as a scale factor for A_{0n}, and consequently has not been included in the quoted errors.

The data at 656 MeV/c are, within the statistical errors, identical to those already published [1], but have slightly smaller error bars for the reasons explained above, and should therefore be preferred. At all energies, the analysing power shows a remarkable angular dependence, with quite large positive values, both in the forward and in the backward regions. The data at 546 MeV/c have a trend very similar to the ones at 656, but considerably smaller errors: in particular, they confirm the large peak in the backward hemisphere. With increasing energy, the main two features of the data are the persistence of the large positive values in the forward region, and the development of a positive structure in the central region.

In Fig. 3, the data are compared with the calculations of some potential models [8-14], and, as in Ref. [1], we have to stress that these models seem to have difficulties in explaining this observable. In particular, it is interesting to note how much the theoretical predictions differ from each other also in the forward hemisphere, where it has been known since a long time [15] that the cross-section is dominated by the π-exchange. This is because A_{0n} is very sensitive to the details of the interaction, and thus to the differences amongst the various models.

At 656 MeV/c the data are shown together with the original predictions of the Paris [12] and Nijmegen [10] models, and with more recent calculations obtained with these models, taking into account the new LEAR data. In the case of the Paris potential, the new fit, obtained through a slight readjustment of the 12 parameters defining the absorptive part of the potential, provides a better agreement with the data in the $\bar{p}p$ elastic channel data, but an even worse disagreement with our data. On the contrary, the explicit use of our data [1] in the

fitting procedure is very constraining for the Nijmegen P-matrix model, and the new fit reproduces even the energy-dependence trend of the data rather well [11].

For completeness, we compare the data at the other three momenta (546, 767, and 875 MeV/c) with the original calculations of Dover and Richard (Model I) [8], the Bonn OBE model [13], and the Myhrer model [9]. The most recent calculations of the Nijmegen P-matrix model are also shown. The first three models treat annihilation in a very simple way with few parameters, and in general the agreement with the data is not too good. At low energy, and in the forward hemisphere, the Myhrer model is quite successful, but as the reaction momentum increases, the agreement with the data rapidly deteriorates, a trend opposite to that observed for this model in the case of the $\bar{p}p$ elastic channel [16].

At present the conclusion is that the meson-exchange potential models tuned on NN data do not satisfactorily reproduce the new A_{0n} data obtained at LEAR in the charge-exchange reaction. Theoretical work is going on, and a very important first point to assess is whether the new $N\bar{N}$ data demand a modification of the generally accepted OBE part of the potential.

Acknowledgements

The construction of the apparatus required a considerable technical effort, and we would like to acknowledge the invaluable contributions of G. Barbier, J. Briatte, P. Ciliberti, J.C. Lugol, F. Maschiocchi, G. Maselli, G. Menon, E. Perrin, J.P. Richeux, L. Simonetti and G. Venier. Some of the authors would like to thank the Swiss National Science Foundation for support. The excellent performance of LEAR made this experiment possible, and we are grateful to J.D. Simon, D. Dumollard, and the LEAR operating staff for their collaboration.

REFERENCES

[1] R. Birsa et al., Phys. Lett. **B246** (1990) 267.

[2] F. Bradamante et al., $N\bar{N}$ scattering experiments: first results from the experiment PS199, Invited talk given at the 4th Conf. on the Intersections between Particle and Nuclear Physics, Tucson, Ariz., 1991.

[3] F. Bradamante, Spin physics at LEAR, Invited talk given at the Workshop on Nucleon–Anti-Nucleon Interactions (NAN '91), Moscow, 1991.

[4] A. Martin et al., Measurement of the analysing power and the differential cross-section of the $\bar{p}p$ charge-exchange reaction, Proc. First Biennial Conference, Stockholm, 1990, eds. P. Carlson et al. (World Scientific, Singapore, 1991), p. 257.

[5] T.O. Niinikoski and F. Udo, Nucl. Instrum. Methods **134** (1976) 219.

[6] A. Amidouch et al., The neutron detectors of the PS199 LEAR experiment, submitted to Nucl. Instrum. Methods (1991).

[7] R. Birsa et al., Nucl. Instrum. Methods **A300** (1990) 43.

[8] C. Dover and J.M. Richard, Phys. Rev. **C21** (1980) 1466.

[9] O.D. Dalkarov and F. Myhrer, Nuovo Cimento **A40** (1977) 152.

[10] J.J. De Swart, private communication (see Ref. [1]).

[11] R.G.E. Timmermans, Th.A. Rijken and J.J. De Swart, An antiproton–proton partial wave analysis, in preparation.

[12] J. Cote et al., Phys. Rev. Lett. **48** (1982) 1319.

[13] T. Hippchen, J. Haidenbauer, K. Holinde and V. Mull, Meson–baryon dynamics in the nucleon–antinucleon system, to be published in Phys. Rev. C.

[14] M. Pignone, M. Lacombe, B. Loiseau and R. Vinh Mau, Recent $\bar{p}p$ data and the Paris $N\bar{N}$ potential, same Proc. as in Ref. [4], p. 90;
R. Vinh Mau, private communication.

[15] R.J.N. Phillips, Rev. Mod. Phys. **39** (1967) 681;
see also the recent analysis of T. Shibata, Phys. Lett. **B189** (1987) 232.

[16] F. Perrot et al., Phys. Lett. **B261** (1991) 188, and private communication.

Table 1
Numerical values obtained in the measurement of the angular distribution of the analysing power at four momenta

$\cos\theta_{cm}$	A_{0n}
546 MeV/*c*	
0.825 ± 0.025	0.272 ± 0.026
0.775 ± 0.025	0.279 ± 0.018
0.725 ± 0.025	0.264 ± 0.017
0.675 ± 0.025	0.197 ± 0.016
0.625 ± 0.025	0.201 ± 0.016
0.550 ± 0.050	0.184 ± 0.013
0.450 ± 0.050	0.164 ± 0.014
0.350 ± 0.050	0.123 ± 0.016
0.250 ± 0.050	0.096 ± 0.018
0.150 ± 0.050	0.089 ± 0.021
0.050 ± 0.050	0.058 ± 0.015
−0.050 ± 0.050	0.017 ± 0.015
−0.150 ± 0.050	0.018 ± 0.017
−0.250 ± 0.050	0.060 ± 0.020
−0.350 ± 0.050	0.012 ± 0.023
−0.450 ± 0.050	0.042 ± 0.025
−0.550 ± 0.050	0.094 ± 0.028
−0.625 ± 0.025	0.163 ± 0.039
−0.675 ± 0.025	0.109 ± 0.041
−0.725 ± 0.025	0.208 ± 0.041
−0.775 ± 0.025	0.218 ± 0.041
−0.825 ± 0.025	0.165 ± 0.043
−0.875 ± 0.025	0.183 ± 0.042

$\cos\theta_{cm}$	A_{0n}
656 MeV/*c*	
0.825 ± 0.025	0.219 ± 0.023
0.775 ± 0.025	0.220 ± 0.015
0.725 ± 0.025	0.206 ± 0.013
0.675 ± 0.025	0.191 ± 0.014
0.625 ± 0.025	0.189 ± 0.015
0.575 ± 0.025	0.151 ± 0.016
0.525 ± 0.025	0.142 ± 0.018
0.475 ± 0.025	0.142 ± 0.019
0.400 ± 0.050	0.130 ± 0.015
0.300 ± 0.050	0.138 ± 0.027
0.150 ± 0.050	0.070 ± 0.028
0.050 ± 0.050	0.026 ± 0.021
−0.050 ± 0.050	0.055 ± 0.030
−0.150 ± 0.050	−0.017 ± 0.039
−0.250 ± 0.050	0.064 ± 0.047
−0.350 ± 0.050	0.046 ± 0.053
−0.450 ± 0.050	−0.114 ± 0.056
−0.550 ± 0.050	0.113 ± 0.063
−0.650 ± 0.050	0.082 ± 0.065
−0.750 ± 0.050	0.170 ± 0.068
−0.825 ± 0.025	0.374 ± 0.102

767 MeV/*c*	
0.825 ± 0.025	0.136 ± 0.022
0.775 ± 0.025	0.166 ± 0.013
0.725 ± 0.025	0.158 ± 0.013
0.675 ± 0.025	0.121 ± 0.013
0.625 ± 0.025	0.136 ± 0.015
0.575 ± 0.025	0.089 ± 0.016
0.525 ± 0.025	0.110 ± 0.018
0.475 ± 0.025	0.109 ± 0.020
0.425 ± 0.025	0.100 ± 0.022
0.375 ± 0.025	0.067 ± 0.026
0.325 ± 0.025	0.025 ± 0.038
0.150 ± 0.050	0.074 ± 0.031
0.050 ± 0.050	0.091 ± 0.027
−0.050 ± 0.050	0.103 ± 0.040
−0.150 ± 0.050	0.109 ± 0.055
−0.250 ± 0.050	0.032 ± 0.063
−0.350 ± 0.050	−0.005 ± 0.067
−0.450 ± 0.050	−0.014 ± 0.073
−0.550 ± 0.050	−0.045 ± 0.074
−0.650 ± 0.050	0.124 ± 0.076
−0.750 ± 0.050	−0.018 ± 0.077
−0.825 ± 0.025	0.142 ± 0.120

875 MeV/*c*	
0.825 ± 0.025	0.149 ± 0.016
0.775 ± 0.025	0.156 ± 0.010
0.725 ± 0.025	0.143 ± 0.009
0.675 ± 0.025	0.138 ± 0.010
0.625 ± 0.025	0.151 ± 0.012
0.575 ± 0.025	0.140 ± 0.013
0.525 ± 0.025	0.139 ± 0.015
0.475 ± 0.025	0.131 ± 0.017
0.425 ± 0.025	0.136 ± 0.019
0.375 ± 0.025	0.132 ± 0.024
0.325 ± 0.025	0.115 ± 0.040
0.175 ± 0.025	0.031 ± 0.050
0.125 ± 0.025	0.147 ± 0.032
0.050 ± 0.050	0.169 ± 0.027
−0.050 ± 0.050	0.240 ± 0.041
−0.150 ± 0.050	0.139 ± 0.055
−0.250 ± 0.050	0.120 ± 0.060
−0.350 ± 0.050	0.083 ± 0.061
−0.450 ± 0.050	−0.091 ± 0.058
−0.550 ± 0.050	−0.063 ± 0.061
−0.650 ± 0.050	−0.073 ± 0.062
−0.750 ± 0.050	0.065 ± 0.062
−0.825 ± 0.025	0.140 ± 0.090

Figure captions

Fig. 1 Schematic layout of experiment PS199: NC labels the neutron counter hodoscopes, ANC the antineutron detectors.

Fig. 2 χ^2 distribution of the kinematical fit (a) and z_{vtx} distribution (b) for polarized target (PT) and dummy target (DT) (hatched histogram) at 875 MeV/c. The ratio $f = B/(B + S)$ for $\chi^2 < 20$ (c) at 656 and (d) at 875 MeV/c.

Fig. 3 Analysing power A_{0n} for $\bar{p}p \rightarrow \bar{n}n$ at four incident $\bar{p}$ beam momenta. The curves are different potential model calculations (see text).

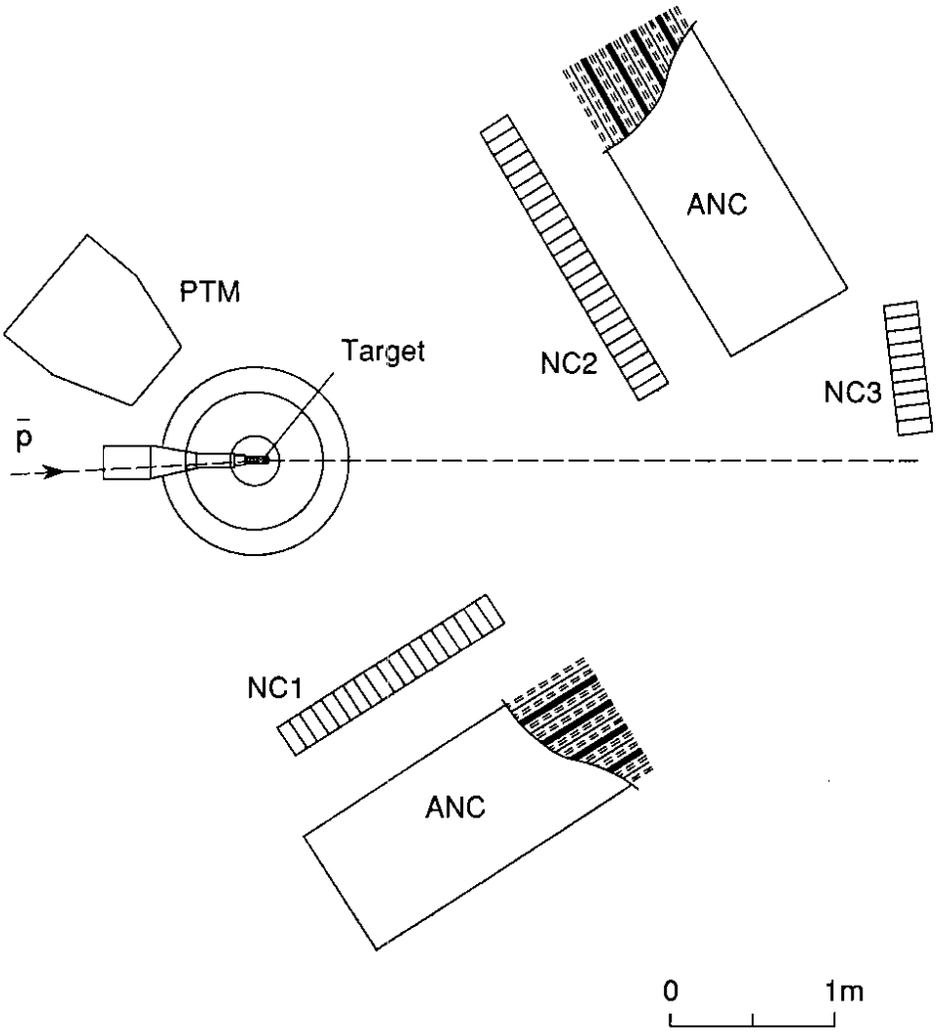

Fig. 1

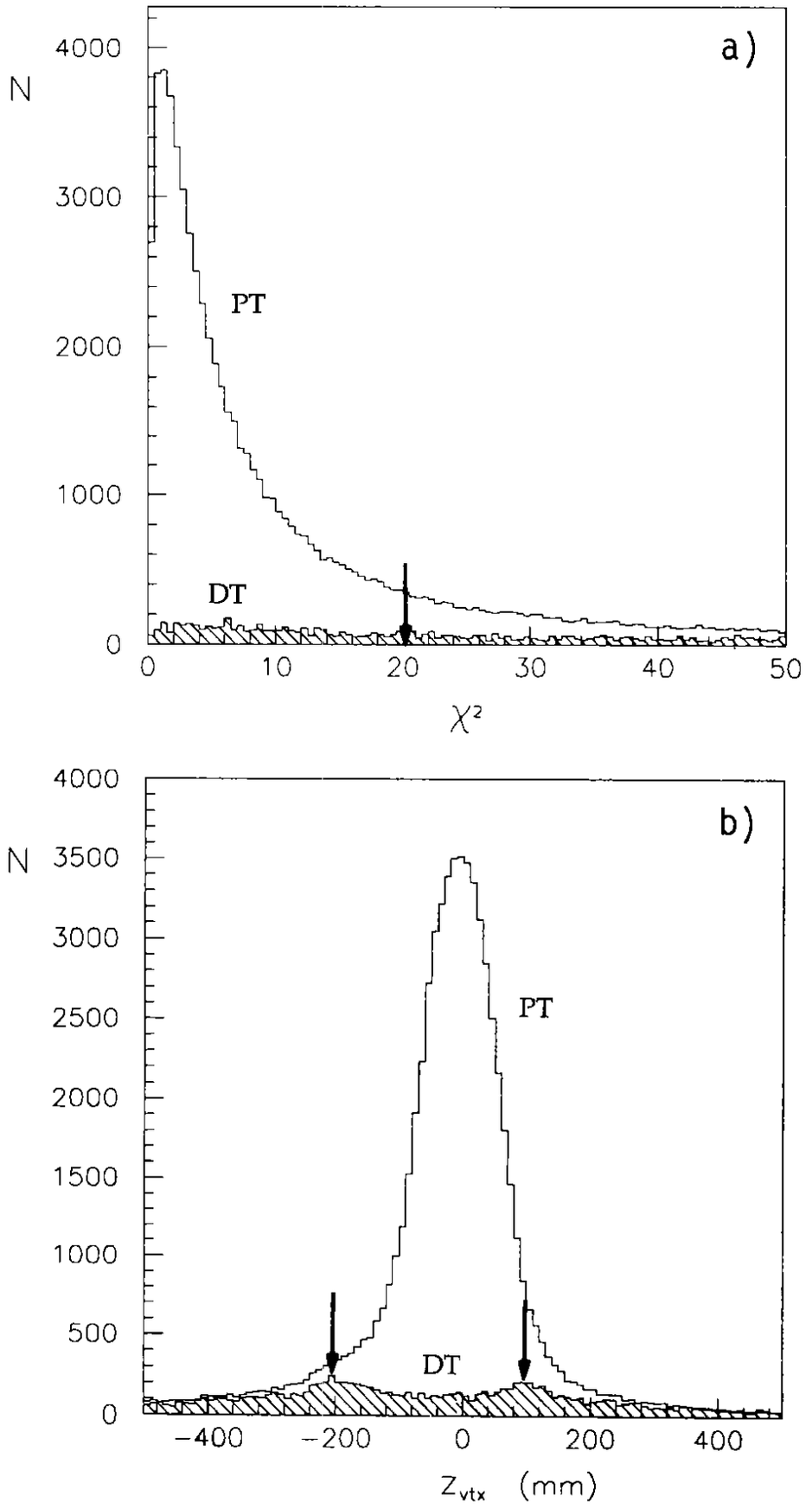
a)
N
4000
3000
2000
1000
0
PT
DT
0
10
20
30
40
50
χ^2
b)
N
4000
3500
3000
2500
2000
1500
1000
500
0
PT
DT
−400
−200
0
200
400
Z_{vtx} (mm)

Fig. 2

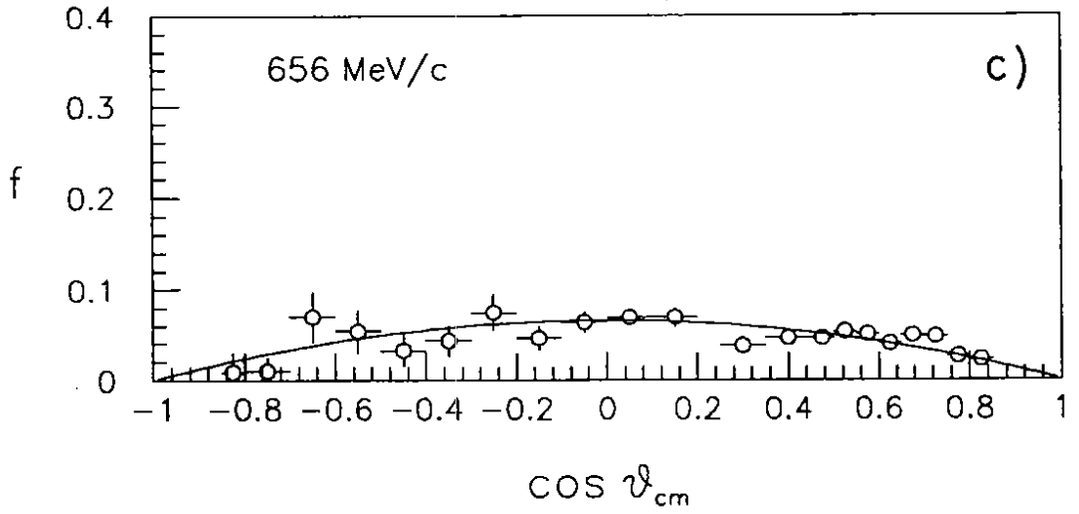
656 MeV/c
c)
f
0.4
0.3
0.2
0.1
0
−1 −0.8 −0.6 −0.4 −0.2 0 0.2 0.4 0.6 0.8 1
cos ϑ_{cm}

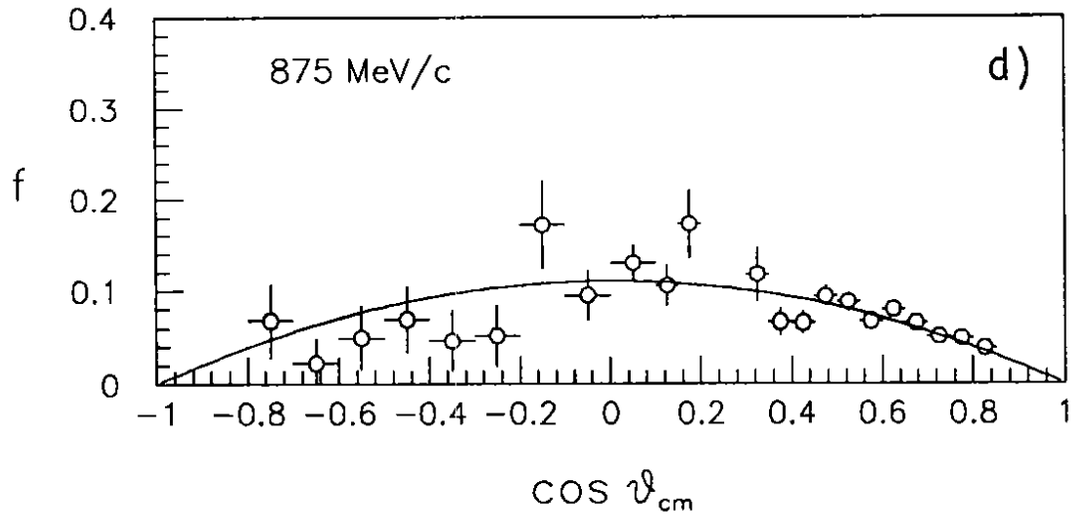
875 MeV/c
d)
f
0.4
0.3
0.2
0.1
0
−1 −0.8 −0.6 −0.4 −0.2 0 0.2 0.4 0.6 0.8 1
cos ϑ_{cm}

Fig. 2 (cont.)

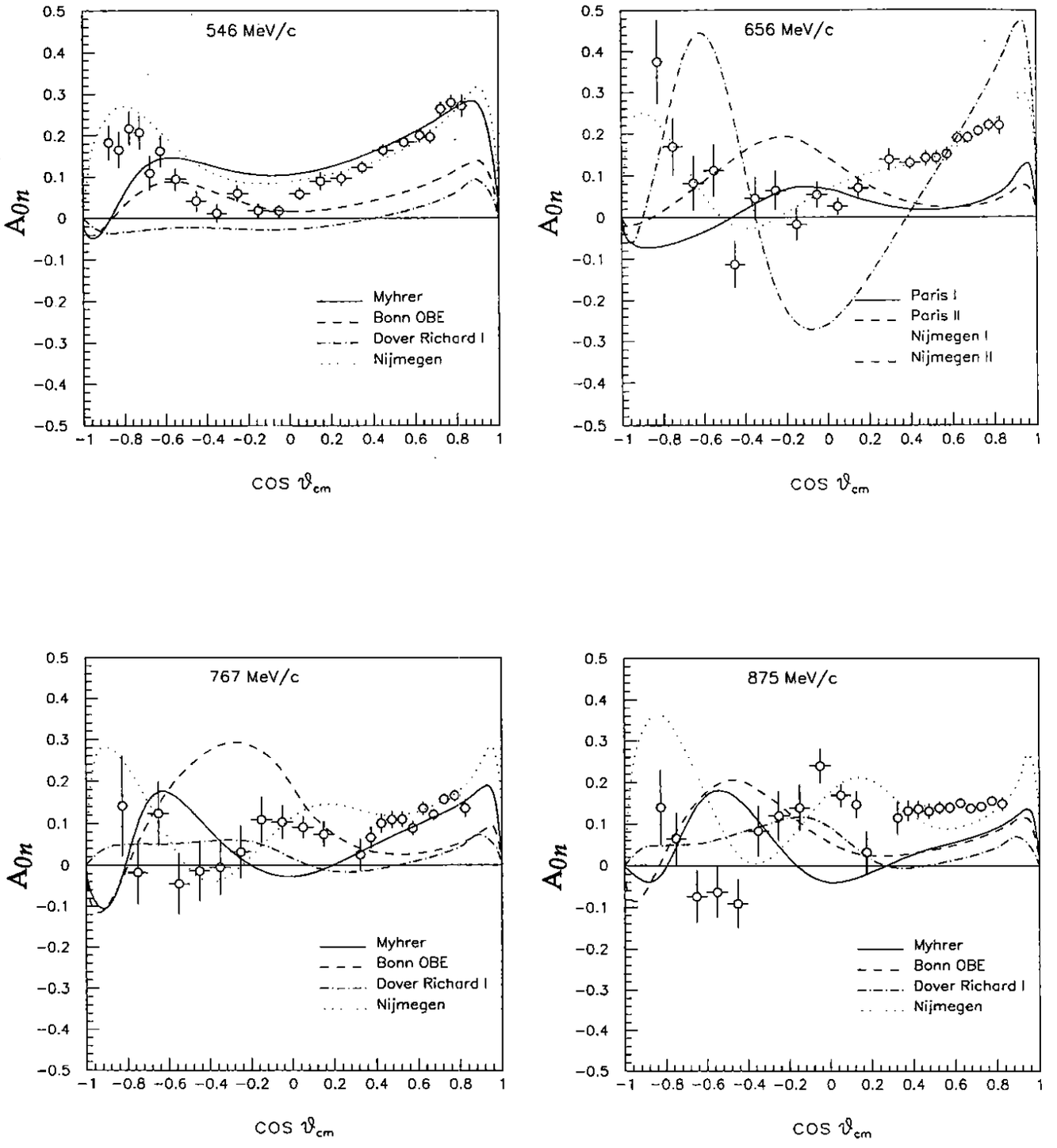

Fig. 3

Imprimé au CERN. Prix : 0.40 Fr.